Available online at www.sciencedirect.com
ScienceDirect
Biochimica et Biophysica Acta 1778 (2008) 937–944
Biochimica et Biophysica Acta
BBA
www.elsevier.com/locate/bbamem

Solution NMR of signal peptidase, a membrane protein

Monika Musial-Siwek, Debra A. Kendall, Philip L. Yeagle *

Department of Molecular and Cell Biology, The University of Connecticut, Storrs, CT 06269, USA

Received 24 July 2007; received in revised form 9 October 2007; accepted 26 November 2007
Available online 14 December 2007

Abstract

Useful solution nuclear magnetic resonance (NMR) data can be obtained from full-length, enzymatically active type I signal peptidase (SPase I), an integral membrane protein, in detergent micelles. Signal peptidase has two transmembrane segments, a short cytoplasmic loop, and a 27-kD C-terminal catalytic domain. It is a critical component of protein transport systems, recognizing and cleaving amino-terminal signal peptides from preproteins during the final stage of their export. Its structure and interactions with the substrate are of considerable interest, but no three-dimensional structure of the whole protein has been reported. The structural analysis of intact membrane proteins has been challenging and only recently has significant progress been achieved using NMR to determine membrane protein structure. Here we employ NMR spectroscopy to study the structure of the full-length SPase I in dodecylphosphocholine detergent micelles. HSQC–TROSY spectra showed resonances corresponding to approximately 3/4 of the 324 residues in the protein. Some sequential assignments were obtained from the 3D HNCACB, 3D HNCA, and 3D HN(CO) TROSY spectra of uniformly ^{2}H, ^{13}C, ^{15}N-labeled full-length SPase I. The assigned residues suggest that the observed spectrum is dominated by resonances arising from extramembraneous portions of the protein and that the transmembrane domain is largely absent from the spectra. Our work elucidates some of the challenges of solution NMR of large membrane proteins in detergent micelles as well as the future promise of these kinds of studies.

Keywords: Signal peptidase; NMR; Membrane protein

1. Introduction

Extensive structural data on soluble proteins are available, but reports on structures of integral membrane proteins with multiple membrane spanning segments still represent less than 1/2% of the database of protein structures [1,2]. Membrane proteins carry out critical physiological functions such as signaling, protein secretion and ion transport, and thus are key targets for drug development. Elucidating the structures of membrane proteins will aid our understanding of their activity, ligand binding sites, and potential interaction with therapeutic agents.

Many difficulties arise when preparing a membrane protein for structural analysis. First, it is challenging to obtain high-yield expression and purification of membrane proteins. A second challenge for membrane protein preparation is the requirement for lipid mimetic environments, such as detergents, to keep these hydrophobic proteins in a native conformation after extraction from their natural environment, the lipid bilayer. Third, it is exceptionally difficult to analyze membrane protein structure with conventional methods such as electron microscopy, X-ray crystallography or NMR spectroscopy. Electron microscopy usually provides only a low-resolution structure of the membrane protein and it is difficult to obtain high quality crystals of proteins from detergent micelles for X-ray analysis. Difficulties with the NMR experiments arise from the large size of many membrane proteins and this leads to relatively slow rotational correlation times and consequent resonance broadening. The overall size of the complex increases when the protein is associated with detergent micelles exacerbating this problem.

NMR spectroscopy on high molecular weight systems has advanced significantly with the introduction of TROSY

Abbreviations: DPC, dodecylphosphocholine; HRMAS, high resolution magic angle spinning; HSQC, heteronuclear single-quantum correlation; NMR, nuclear magnetic resonance; OG, *n*-octyl-β-D-glucopyranoside; SPase I, type I signal peptidase

* Corresponding author. Department of Molecular and Cell Biology, 91 North Eagleville Road, The University of Connecticut, Storrs, CT 06269, USA. Tel.: +1 860 486 5154.
E-mail address: yeagle@uconn.edu (P.L.Yeagle).

0005-2736/$ - see front matter © 2007 Elsevier B.V. All rights reserved.
doi:10.1016/j.bbamem.2007.11.013

experiments [3]. TROSY has enabled the NMR analysis of larger proteins than was previously possible. Using this NMR methodology several membrane protein structures have been investigated (for review see [4]). A number of structures of β-barrel proteins from bacterial outer membranes (up to 20 kD) have been analyzed using NMR techniques [5–7]. Structures of integral membrane proteins solubilized in organic solvents have also emerged [8,9], although organic solvents might be unsuitable for proteins with large extramembraneous segments [2]. Using NMR methods, some structural data have been obtained from integral membrane protein structures containing multiple helical transmembrane segments [10–14]. However, only one complete chemical shift assignment of an intact integral membrane protein with a transmembrane helical bundle in detergent micelles has been reported thus far [15], and no complete three-dimensional structures have yet been reported in the literature.

Here we use *Escherichia coli* signal peptidase I (SPase I) as a model membrane-bound protein for the development of methods for NMR structural determination. SPase I is found in the membranes of Gram-negative and Gram-positive bacteria, the endoplasmic reticulum (ER), chloroplast, and mitochondria (for reviews see [16–18]). The enzyme cleaves the amino-terminal signal peptide from a secreted protein during the final stages of membrane translocation and consequently, plays a critical role in protein targeting.

SPase I is a protein with two transmembrane segments (residues 4–28 and 58–76), a cytoplasmic loop (residues 29–57), and a periplasmic C-terminal catalytic domain (residues 77–323). Although a crystal structure of the soluble C-terminal catalytic domain of the SPase I has been reported [19–21], there is no structural information on the full-length protein. Therefore, the structural relationship between the catalytic domain and the transmembrane domain is unknown.

Here we report solution NMR data from full-length SPase I, including the transmembrane domain. We expressed, isotopically labeled, and purified the protein in quantity sufficient for NMR analysis at 600 MHz and 900 MHz. The SPase I was active under the conditions of the NMR experiment. Data from uniformly ^{2}H, ^{13}C, ^{15}N-labeled intact SPase I show interpretable ^{1}H–^{15}N TROSY–HSQC, HNCACB, HNCA and HN(CO) NMR spectra. The most readily visible resonances arise from the large C-terminal domain of the protein.

2. Materials and methods

2.1. Materials

Deuterium oxide (99.9%), ammonium chloride (>99% ^{15}N-labeled), and glucose (uniformly >99% ^{13}C-labeled) were purchased from Spectra Stable Isotopes (Columbia, MD). Dnase I (Amplification Grade) was obtained from Invitrogen Corp. (Carlsbad, CA), *n*-octyl-β-D-glucopyranoside (OG) (Calbiochem, La Jolla, CA), dodecylphosphocholine (DPC) (Avanti, Polar Lipids, Inc., Alabaster, AL), Q-Sepharose (GE Healthcare, Piscataway, NJ), and Ni-agarose were from Qiagen (Valencia, CA).

2.2. Signal peptidase expression and purification

BL21(DE3) cells transfected with the pET23b plasmid (generously provided by Ross Dalbey, The Ohio State University), coding for *E. coli* 6-His-tagged SPase I, were grown in M9 Minimal Media labeled with ^{2}H, ^{13}C and ^{15}N (^{2}H, ^{13}C, ^{15}N-M9 media): 99.9% D_2O, 11.1 mM ^{13}C-labeled glucose, and 18.7 mM ^{15}N-labeled ammonium chloride. First, the cells were grown in 25 ml of 50%/50% $^{2}H/^{1}H$, ^{13}C, ^{15}N-M9 media overnight to reach OD=0.7, then 20 ml of cells were spun for 10 min at 13,000 rpm sterilely and resuspended in 50 ml ^{2}H, ^{13}C, ^{15}N-M9 media. The cells were grown to reach OD_{600}=0.84, spun again sterilely for 10 min at 13,000 rpm and resuspended in 500 ml ^{2}H, ^{13}C, ^{15}N-M9 media. Starting with OD_{600}=0.18 the cells were grown at 37 °C with shaking at 230 rpm until OD_{600}=0.5 followed by induction with 0.5 mM IPTG for 4 h. Cells were harvested by centrifugation at 6000 rpm for 20 min, and resuspended in 25 ml of lysis buffer (50 mM Tris, pH 8.0, 20% glucose). The solution was mixed, after addition of lysozyme (6 mg) and Dnase I, for 10 min at room temperature and frozen at −70 °C overnight. The labeled SPase I was purified as described previously by Klenotic et al. [22] with some modifications. Cells were thawed and 200 μl of 1 M magnesium acetate was added to the sample. The sample was mixed, centrifuged, and the pellet resuspended in 10 mM triethanolamine, 10% glycerol, pH 7.9. Following centrifugation, the pellet was homogenized in solubilization buffer (10 mM triethanolamine, 10% glycerol, 1% Triton X-100, pH 7.9), centrifuged again and the supernatant loaded on a Q-Sepharose column. The SPase I was eluted with a continuous gradient of 0–0.1 M KCl. Fractions containing SPase I were loaded onto Ni-agarose resin equilibrated in 6-His buffer (10 mM Tris, pH 8.5, 100 mM KCl, 20 mM imidazole, 10 mM B-mercaptoethanol, and 1% Triton X-100) and eluted with a step gradient of imidazole (100–300 mM). To remove the imidazole and prepare the sample for NMR spectroscopy, the protein was concentrated and buffer exchanged with 20 mM phosphate buffer pH 6.3, 10 mM EDTA (added to negate possible Ni interference) and 0.3% Triton X-100 using a Centricon-10 membrane (Millipore, Billerica, MA). Protein concentration was determined with the BCA Protein Assay Kit (Pierce, Rockford, IL).

2.3. Detergent exchange

To exchange detergents, the Ni-agarose resin bound with SPase I was washed 3 times with 1% of one of the three detergents, Triton X-100, OG, or DPC in 6-His buffer and spun at very low speed (1000 rpm) to separate the resin-bound protein from the buffer. SPase I was eluted with four washes of 300 mM imidazole. To remove the imidazole and prepare sample for the NMR, the protein was concentrated and buffer exchanged with 20 mM NaH_2PO_4 pH 6.3, 10 mM EDTA and the appropriate detergent using a Centricon-10 membrane. SPase I in each detergent was incubated at 22 °C and 37 °C for one week and checked for stability by monitoring for degradation products on SDS-PAGE gels and by testing the activity (see below).

2.4. Activity assay

GST fused to the N-terminus of the alkaline phosphatase signal peptide (SP) and first 30 amino acids of the mature protein (AP), and 6-His-tagged (His) at the C-terminus (GST–SP–AP–His), was used as a substrate for SPase I proteolysis [23]. Signal peptidase was incubated at different concentrations with GST–SP–AP–His in Tris buffer pH 8, and 1% Triton X-100, or 1% OG, or 1% DPC at 37 °C for 2 h. The reaction was stopped by addition of sample buffer. The sample was run on SDS-PAGE and silver stained.

2.5. NMR experiments

All experiments were performed on either a 900 MHz Bruker or a 600 MHz Varian spectrometer at 22 °C. 2D ^{1}H–^{15}N TROSY–HSQC, 3D HNCACB, 3D HNCA and 3D HN(CO) spectra were collected on ^{2}H, ^{13}C, ^{15}N-labeled SPase I at 12 mg/ml in 20 mM NaH_2PO_4, 10 mM EDTA, pH 6.3 and 1% DPC. This detergent concentration was well above the critical micelle concentration for DPC and from the molar ratio (DPC/SPase I is about 93) it can be estimated that about 1 protein molecule, on average, was in each detergent micelle. The ^{1}H–^{15}N HSQC spectra were acquired as 2048 and 128 complex points in ^{1}H and ^{15}N dimension, respectively. For the SPase I sequence specific assignments, a combination of 3D HNCACB, 3D HNCA and 3D HN(CO) spectra was utilized. 3D HNCACB data were acquired with 1024 points in the ^{1}H dimension, 64 points in the ^{15}N dimension, and 32 points in the ^{13}C dimension, while being

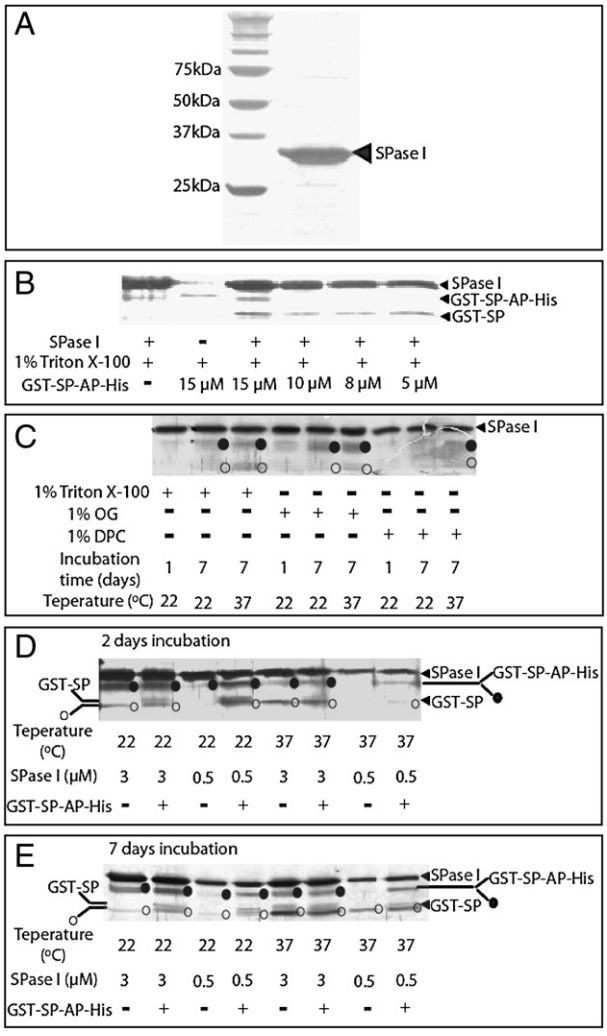

Fig. 1. Analysis of *E. coli* SPase I stability and activity under different conditions. (A) Silver-stained SDS-PAGE of purified SPase I indicating the enzyme is about 95% pure. (B) Analysis of SPase I activity on silver stained SDS-PAGE. Different concentrations, as indicated, of the substrate (GST–SP–AP–His) were incubated with 1 µM SPase I over 2 h at 37 °C. The location of SPase I, GST–SP–AP–His, and the cleavage product, GST–SP, is indicated on the gel. (C) Comparison of the degradation of SPase I in Triton X-100, OG, and DPC detergent micelles via silver stained SDS-PAGE. Incubation time and temperature are indicated. The band corresponding to SPase I is marked and two of the degradation products are indicated by ● and ○. While, some discoloring is present on the scanned image in the last lane, the bands still can be distinguished. (D) Analysis of SPase I activity conducted as in (B). SPase I was incubated over 2 days in DPC micelles at different temperatures, as indicated, prior to the activity analysis. The band corresponding to SPase I is marked and two of the degradation products are indicated by ● and ○. (E) Analysis of SPase I activity conducted as in (B). SPase I was incubated over 7 days in DPC micelles at different temperatures, as indicated, prior to the activity analysis. The band corresponding to SPase I is marked and two of the degradation products are indicated by ● and ○.

averaged over 8 transients. 3D HNCA were acquired with 1024 points in the ^{1}H dimension, 64 points in the ^{15}N dimension, and 16 points in the ^{13}C dimension over 16 transients. 3D HN(CO) data were acquired with 1024 points in the ^{1}H dimension, 64 points in the ^{15}N dimension, and 16 points in the ^{13}C dimension over 16 transients. All spectra were processed using nmrPipe/nmrDraw software [24] and analyzed using the program Sparky (http://www.cgl.ucsf.edu/home/sparky).

3. Results

3.1. Isolation of stable-isotope labeled SPase I

Since NMR is a relatively insensitive technique, an expression system that provides a high yield of membrane protein labeled with stable isotopes is critical. Therefore, the production of SPase I from BL21 (DE3) cells transfected with the pET23b-coding SPase I plasmid, in LB media, then in minimal media, was optimized. Subsequently, the expression of SPase I was examined in minimal media in the presence of deuterium oxide (D_2O). No significant difference in expression levels was observed in the presence and absence of D_2O, although the cells grew much more slowly in D_2O. For example, to reach OD_{600} of 0.5 the growth time increased by 40% in minimal media and 70% in minimal media containing D_2O, compared to the cell growth in LB media. We found that adaptation of the cells to the D_2O containing media was unnecessary. We also explored different induction times and found that a point, intermediate in log phase, was critical in maximizing expression level and minimizing degradation of the expressed protein. In addition, there was no difference observed in SPase I expression in the presence of different percentages of D_2O, or when MOPS media was used instead of M9 media. It proved possible to obtain 8.75 mg (12 mg/ml) of protein from 2 L of ^{2}H, ^{13}C, ^{15}N-labeled M9 media at about 95% purity (Fig. 1A).

3.2. Activity of purified, stable-isotope labeled SPase I

The activity of the stable-isotope labeled SPase I was monitored using an established assay [22,25]. In this assay, SPase I recognizes the signal peptide of the GST–SP–AP–His construct and cleaves the assembly into two fragments (C-terminal to the −1 position of the signal peptide). The two fragments are: (1) the GST protein plus the signal peptide (28 kD), and (2) the first 30 amino acids of the mature region 6-His-tagged (4 kD). On the gel, the appearance of the GST–SP band (28 kD) becomes evident, while the intensity of the band corresponding to the GST–SP–AP–His (32 kD) decreases in the presence of the enzyme relative to without the enzyme (Fig. 1B). These observations indicate that the GST–SP–AP–His fusion protein is cleaved by SPase I and reveal that the enzyme activity of the expressed protein is comparable to previously published assays [22,25]. Interestingly, the enzyme is more rapidly proteolyzed in the presence of the substrate, which would indicate that the GST–SP–AP–His activates the enzyme to some extent.

3.3. Detergent and temperature effects on protein stability

Because NMR experiments require long collection times, it is critical to find conditions under which the protein is stable for the duration of NMR data collection. We investigated three detergents (Triton X-100, OG and DPC) to determine which type of detergent micelles are better suited to maintain the stability of SPase I. Triton X-100 is a detergent often used to solubilize membrane proteins and SPase I is active in this detergent [26]. However, SPase I is unstable in Triton X-100

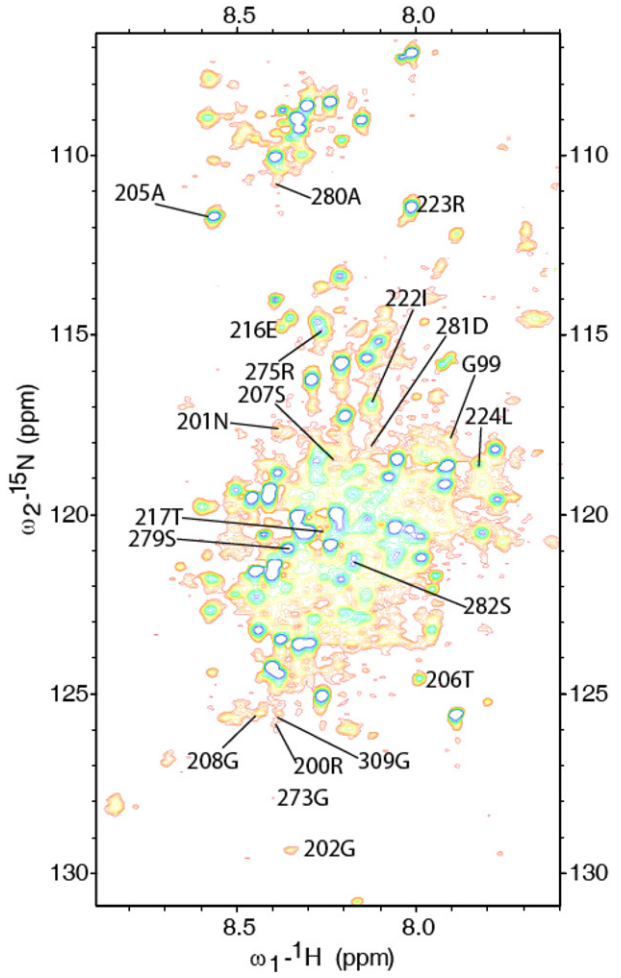

Fig. 2. ^{1}H, ^{15}N-TROSY–HSQC spectrum at 600 MHz (^{1}H) of 0.3 mM uniformly ^{2}H, ^{13}C, ^{15}N-labeled SPase I in DPC micelles at pH 6.3 and 22 °C. Peaks that were identified, as described in the text, are labeled.

when incubated for a long time at elevated temperature. For example, after incubating the sample at 30 °C over 24 h white precipitate could be seen. Consistent with our observations, Wang et al. [27] established that SPase I is autolysed to a greater extent in Triton X-100 than in lipid vesicles (50% PC:50% PE).

The extent of SPase I degradation and its activity was tested in the presence of other detergent micelles. Another detergent previously used successfully to purify the enzyme was 1% OG [22]. Therefore this detergent (1%) and a detergent commonly used for NMR experiments with membrane proteins, 1% DPC [15], were both tested for their ability to maintain stable SPase I and were compared with 1% Triton X-100. From Fig. 1C it is apparent that SPase I is degraded in the presence of all three detergents, Triton X-100, OG and DPC, over time (e.g. compare 1 and 7 day incubations at 22 °C). The slowest degradation occurred in DPC. Elevated temperature enhances enzyme degradation: at 37 °C, the protein is autolysed and degraded more than at 22 °C (e.g. a lower molecular weight degradation product becomes evident). At 37 °C, degradation occurred to a lesser extent in DPC micelles than in Triton X-100 or OG. It has been reported that the autolysis site is located between two helices, at Ala40 and Ala41, consistent with our observation, generating a 31.5-kD size fragment after the cleavage [27]. SPase I activity was comparable in all three detergents (data not shown). Therefore, the following experiments were carried out with SPase I in DPC detergent micelles.

The temperature-dependent degradation and loss of SPase I activity in DPC micelles was determined. Temperature is important for the NMR experiment. Large complexes tumble very slowly leading to broadening of the NMR signal. The rotational correlation time of the protein in solution decreases with increase in temperature. Therefore, increasing the temperature would be expected to narrow resonances, resulting in a better-resolved NMR spectrum. However, the disadvantage of higher temperature is that SPase I is activated at higher temperature escalating the autolysis and leading to loss of enzyme activity. Consequently, we analyzed the enzyme activity after incubation as a function of time at 22 °C and 37 °C. In Fig. 1D and E, the predominant band at the molecular weight corresponding to SPase I was evident. Autolysed SPase I (marked with a closed circle and co-migrating with the substrate) and bands at lower molecular weight (marked with an open circle), indicating degradation of the protein, appeared after two days and became

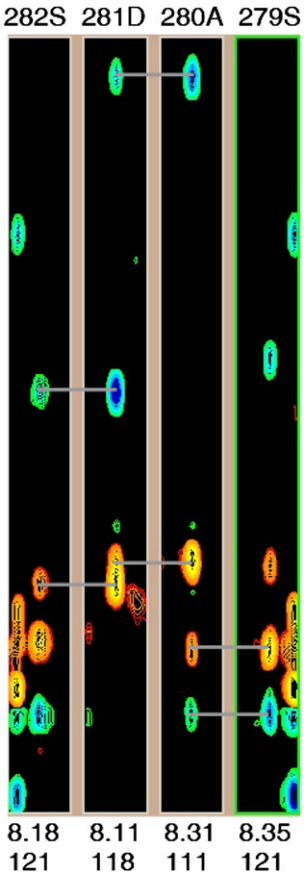

Fig. 3. Sequential assignment of SPase I residues. Some of the strip plots acquired from the HNCACB experiment are shown with residues/numbers indicated above the plots and chemical shifts shown at the bottom of the plot for ^{1}H and ^{15}N and on the side for ^{13}C. The C^{α} (orange) and C^{β} (blue) have opposite signs. Correlated peaks are connected with lines.

Table 1
Sequential resonance assignment of uniformly ^{2}H, ^{13}C, ^{15}N-labeled SPase I amino acid sequence from chemical shifts observed in NHCACB and NHCA experiments

			i		i-1	
Residue	^{15}N (ppm)	NH (ppm)	C^{α} (ppm)	C^{β} (ppm)	C^{α} (ppm)	C^{β} (ppm)
99G	118.3	7.96	44.76	NA	61.1	37.8 (98I)[a]
110G	127.3	8.21	45.17	NA	61.5	37.6 (109Y)[a]
202G	128.3	8.35	45.13	NA	53.3	38.7
201 N	116.4	8.38	53.3	38.5	44.9	29.4
200R	126.8	8.38	44.9	29.7	ND	ND
208G	126.8	8.44	44.9	NA	58.5	64
207S	119.2	8.25	58.5	63.8	61.4	69.3
206T	124.9	8.06	61.35	69.2	52.5	18.5
205A	112.6	8.45	52.4	18.5	56.1	29.6 (204E)[a]
217T	120.4	8.26	61.57	69.1	56.04	29.6
216E	114.9	8.4	56.1	29.6	52.85	38.5 (215N)[a]
224L	118.4	7.84	61.8	37.5	56.6	29.7
223R	110.6	7.94	56.4	29.8	61.1	37.6
222I	116.4	8.1	61.1	37.7	45	NA (221G)[a]
273G	127.5	8.37	45	NA	55.9	32.6 (272M)[a]
275R	115.6	8.29	55.97	29.7	52.6	38.2 (274N)[a]
282S	121.1	8.18	58.3	63.4	54.2	40.75
281D	118.3	8.105	54	40.7	52.4	18.4
280A	111.1	8.31	52.9	18.65	58.8	63.5
279S	120.7	8.34	58.9	63.4	53	38.4 (278N)[a]
309G	126.8	8.38	44.9	NA	56.3	29.7 (308E)[a]

[a]No peaks for its own C^{α} and C^{β} resonances were detected.

more predominant after seven days of incubation. These signs of degradation were more prominent at 37 °C with autolysed SPase I further degrading to smaller fragments. After seven days of incubation, some fraction of the enzyme remained active at either temperature though less full-length enzyme was available at 37 °C. To ensure that the quality of the sample did not vary significantly in different experiments collected at different times following the purification of the protein, the temperature used to collect the NMR data was 22 °C.

3.4. HSQC spectrum of signal peptidase

High-resolution NMR spectra were obtained from intact SPase I in DPC detergent micelles. Fig. 2 shows the 600 MHz ^{1}H–^{15}N TROSY–HSQC spectrum of uniformly ^{2}H, ^{13}C, ^{15}N-labeled SPase I in DPC micelles. (The ^{1}H–^{15}N TROSY–HSQC spectrum acquired on the 900 MHz spectrometer did not differ substantially from the spectrum acquired on the 600 MHz instrument (data not shown).) In the 2D ^{1}H–^{15}N HSQC, many modestly resolved peaks were observed. Among these, approximately 24 Gly peaks were observed in the area of the HSQC spectrum where Gly residues were expected. In the SPase I amino acid sequence there are 28 Gly residues and of these, 4 Gly residues are located in the transmembrane segments.

The sample was also examined with magic angle spinning (MAS) NMR spectroscopy. MAS NMR has been used extensively to study membrane proteins in membrane bilayers [28–32]. Considering the size of SPase I in association with detergent micelles and the fact that large complexes do not tumble rapidly in solution, we combined solution NMR with MAS NMR to determine whether high resolution MAS (HRMAS) would increase resolution of the resonances. Comparison of HRMAS ^{1}H, ^{15}N 2D-HSQC (on a 500 MHz spectrometer) with static ^{1}H, ^{15}N 2D-HSQC (on a 600 MHz spectrometer), revealed no detectable improvement in resolution (data not shown).

3.5. Sequential resonance assignment

Collection and analysis of 3D HNCACB, 3D HNCA and 3D HN(CO) experiments allowed us to sequentially assign segments of the protein amino acid sequence using ^{2}H, ^{13}C, ^{15}N-labeled samples. In Fig. 3, selected ^{15}N planes of sequential NMR spin system connectivities from a 600 MHz 3D HNCACB spectrum of uniformly ^{2}H, ^{13}C, ^{15}N-labeled SPase I are shown. From these data it was possible to sequentially assign sets of contiguous residues as follow: 98I–99G, 109Y–110G, 200R–202G, 205A–208G, 215N–217T, 221G–224L, 272M–275R, 278N–282S, and 308E–309G (Table 1).

4. Discussion

Little is known about the three-dimensional structures of transmembrane proteins. Only about 0.5% of the structures in the Protein Data Bank are of transmembrane proteins because of the difficulty of crystallizing membrane proteins [2]. This dearth of structural information signals a need for alternative means for determination of membrane protein structure.

NMR has yet to make a large contribution to the collective knowledge of the complete three-dimensional structures of membrane proteins. Solid state NMR techniques have been used to considerable advantage in the study of membrane proteins [33–40], but no complete membrane protein structures have been reported by solid state NMR except for structures based on one transmembrane helix. Ordinary solution NMR is handicapped by the

lack of solubility in aqueous media of membrane proteins. To circumvent this problem, a large number of studies of membrane protein fragments in both aqueous and organic media have now been reported [41–61]. These studies have provided extensive information on the secondary structure of the fragments, which in turn have been shown to report on the secondary structure of the intact protein. These studies by themselves cannot provide extensive three-dimensional information. However, it has been possible to successfully combine such experimental information of secondary structure with non-NMR experimental distance data to develop moderate resolution structures for entire integral membrane proteins [62].

The greatest success from solution NMR studies so far has been with the bacterial porins, which are formed of β-barrels. Complete three-dimensional structures have now been reported for several porins from high resolution solution NMR data [5,6,63–66]. More recently, backbone assignments of KcsA in SDS micelles [67] and studies on diacylglycerol kinase with three transmembrane segments per monomer have been reported [15].

In this study, we have made some progress in the structure analysis of the SPase I, an integral membrane protein with two transmembrane segments, using solution NMR techniques. The NMR data indicate that it is feasible to obtain structural information on large membrane proteins. The acquired NMR spectra of the intact SPase I show moderate resolution under conditions in which SPase I activity is maintained. Remarkably, considering the size of the SPase I–detergent micelle complex, about 75% of SPase I residues gave rise to resonances in the 2D ^{1}H–^{15}N HSQC spectrum. Moreover, some of these resonances were assigned, using a combination of HNCACB, HNCA, and HN(CO) experiments of uniformly ^{2}H, ^{13}C, ^{15}N-labeled SPase I (Table 1). This suggests that in addition to the TROSY experiment, which enhances the quality of the observed NMR spectra, application of a more sensitive CBCA(CO)NH experiment, might lead to better resolution of the NMR data and therefore increase the number of assigned residues.

All of the assigned segments of the uniformly ^{2}H, ^{13}C, ^{15}N-labeled SPase I were located in the catalytic extramembraneous domain of the protein. The count of observable Gly residues was consistent with the visualization of only the extramembraneous domain of the protein. Therefore it appears that the NMR spectrum arises almost entirely from the C-terminal extramembraneous domain of the SPase I, with little or no contribution from the transmembrane domain of this protein. There are two possible explanations for this observation. First, the presence of the ^{2}H isotope affects the NMR experiments because the peptide backbone of the transmembrane segments (inside the detergent micelle) does not back exchange for ^{1}H due to the stability of the transmembrane α-helices, while the more exposed backbone of the β-sheet in the extramembraneous domain does. Under the simplifying assumption that the amide protons not observed are actually deuterons that have not efficiently exchanged with protons, the NMR data indicate that an upper limit of about 25% of the amides has not exchanged. This number is close to the estimate of about 30% of the protein's residues in the transmembrane domain. This suggestion is consistent with the slow ^{1}H–^{2}D exchange expected from the stable helices of a transmembrane domain in a hydrophobic environment (interior of a detergent micelle). Second, the transmembrane helices within the detergent micelle are conformationally rigid and only experience the correlation time of the rotational diffusion of the detergent micelle, while the extramembraneous domain may experience some independent motion, leading to some additional averaging of dipolar interactions in the latter case. Some improvement might then be expected at higher temperature, which can lead to shorter rotational correlation times of the ensemble. However we found that the protein is degraded substantially at higher temperatures; therefore the temperature was maintained at 22 °C during the time of acquisition. Increasing field strength should increase the resolution and produce better data. However we compared the data from a 900 MHz spectrometer, which is the highest field strength available, with the data from a 600 MHz spectrometer and cold probe, both with TROSY, and observed little improvement in resolution for this protein at the higher field strength. The TROSY effect is modest even at high field and the MAS experiments did not yield significant improvement in linewidths. These observations suggest that in this particular membrane protein, contrary to expectations, internal motions in the extramembraneous domain may play a significant role in determining linewidth and resolution.

NMR chemical shifts have a strong correlation with the secondary structure of a protein [68,69]. The method presented by Wang et al. provides a fast and reliable way to identify secondary structure based on the NMR chemical shifts [70]. They introduced a new approach, called Probability Based Secondary Structure Identification, to identify protein secondary structure from NMR chemical-shift data. To predict secondary structure of identified SPase I segments, C^{α} was compared to the chemical shifts categorized according to secondary structure type as calculated by Wang et al. We found that most chemical shifts observed for intact SPase I correspond to β-strand or random coil in agreement with the known crystal structure of the SPase I catalytic domain. This analysis is consistent with the SPase I in its native configuration, consistent with the activity data.

Further work on the whole structure of SPase I is in progress. Since detergents other than the DPC used in this study have been shown to provide a better NMR spectrum [71], we are currently examining the activity and stability of SPase I in diverse detergent micelles. In addition, it would be useful to obtain NMR data from SPase I in complex with its inhibitor. The high rate of enzyme autolysis at elevated temperature might be reduced with the presence of the inhibitor, acting as the competitor. Binding of the inhibitor might also stabilize the enzyme, and ensure that the enzyme is in native conformation; consequently NMR experiments might be acquired at higher temperature resulting in better resolved spectra.

Acknowledgements

We thank Klaas Hallenga (National Magnetic Resonance Facility at Madison, University of Wisconsin—Madison) for

collection of NMR data on the 900 MHz spectrometer, Gregory Choi (Structural Biology, University of Connecticut) the for help in the collection of NMR data on the 600 MHz spectrometer and Patricia Wilkinson of Bruker BioSpin Corporation (Billerica, MA) for the HRMAS experiments. This research was supported in part by National Institutes of Health Grant GM37639 (to D.A.K.) and in part by National Institutes of Health Grant GM65250 (to P.L.Y.).

References

[1] C. Tian, M.D. Karra, C.D. Ellis, J. Jacob, K. Oxenoid, F. Sonnichsen, C.R. Sanders, Membrane protein preparation for TROSY NMR screening, Methods Enzymol. 394 (2005) 321–334.
[2] C.R. Sanders, F. Sonnichsen, Solution NMR of membrane proteins: practice and challenges, Magn. Reson. Chem. 44 (2006) S24–S40.
[3] K. Pervushin, R. Riek, G. Wider, K. Wuthrich, Attenuated T2 relaxation by mutual cancellation of dipole–dipole coupling and chemical shift anisotropy indicates an avenue to NMR structures of very large biological macromolecules in solution, Proc. Natl. Acad. Sci. U. S. A. 94 (1997) 12366–12371.
[4] L.K. Tamm, B. Liang, NMR of membrane proteins in solution, Prog. NMR Spectrosc. 48 (2006) 201–210.
[5] C. Fernandez, K. Wuthrich, NMR solution structure determination of membrane proteins reconstituted in detergent micelles, FEBS Lett. 555 (2003) 144–150.
[6] A. Arora, F. Abildgaard, J.H. Bushweller, L.K. Tamm, Structure of outer membrane protein A transmembrane domain by NMR spectroscopy, Nat. Struct. Biol. 8 (2001) 334–338.
[7] P.M. Hwang, W.Y. Choy, E.I. Lo, L. Chen, J.D. Forman-Kay, C.R. Raetz, G.G. Prive, R.E. Bishop, L.E. Kay, Solution structure and dynamics of the outer membrane enzyme PagP by NMR, Proc. Natl. Acad. Sci. U. S. A. 99 (2002) 13560–13565.
[8] I.L. Barsukov, G.V. Abdulaeva, A.S. Arseniev, V.F. Bystrov, Sequence-specific 1H-NMR assignment and conformation of proteolytic fragment 163–231 of bacterioopsin, Eur. J. Biochem. 192 (1990) 321–327.
[9] M. Schwaiger, M. Lebendiker, H. Yerushalmi, M. Coles, A. Groger, C. Schwarz, S. Schuldiner, H. Kessler, NMR investigation of the multidrug transporter EmrE, an integral membrane protein, Eur. J. Biochem. 254 (1998) 610–619.
[10] K.R. MacKenzie, J.H. Prestegard, D.M. Engelman, A transmembrane helix dimer: structure and implications, Science 276 (1997) 131–133.
[11] M.E. Girvin, V.K. Rastogi, F. Abildgaard, J.L. Markley, R.H. Fillingame, Solution structure of the transmembrane H^+-transporting subunit c of the F1F0 ATP synthase, Biochemistry 37 (1998) 8817–8824.
[12] V.K. Rastogi, M.E. Girvin, ^{1}H, ^{13}C, and ^{15}N assignments and secondary structure of the high pH form of subunit *c* of the F1F0 ATP synthase, J. Biomol. NMR 13 (1999) 91–92.
[13] M.F. Mesleh, S. Lee, G. Veglia, D.S. Thiriot, F.M. Marassi, S.J. Opella, Dipolar waves map the structure and topology of helices in membrane proteins, J. Am. Chem. Soc. 125 (2003) 8928–8935.
[14] C. Tian, R.M. Breyer, H.J. Kim, M.D. Karra, D.B. Friedman, A. Karpay, C.R. Sanders, Solution NMR spectroscopy of the human vasopressin V2 receptor, a G protein-coupled receptor, J. Am. Chem. Soc. 127 (2005) 8010–8011.
[15] K. Oxenoid, H.J. Kim, J. Jacob, F.D. Sonnichsen, C.R. Sanders, NMR assignments for a helical 40 kDa membrane protein, J. Am. Chem. Soc. 126 (2004) 5048–5049.
[16] H. Tjalsma, A.G. Stover, A. Driks, G. Venema, S. Bron, J.M. van Dijl, Conserved serine and histidine residues are critical for activity of the ER-type signal peptidase SipW of *Bacillus subtilis*, J. Biol. Chem. 275 (2000) 25102–25108.
[17] M. Paetzel, A. Karla, N.C. Strynadka, R.E. Dalbey, Signal peptidases, Chem. Rev. 102 (2002) 4549–4580.
[18] R. Tuteja, Type I signal peptidase: an overview, Arch. Biochem. Biophys. 441 (2005) 107–111.
[19] M. Paetzel, J.J. Goodall, M. Kania, R.E. Dalbey, M.G. Page, Crystallographic and biophysical analysis of a bacterial signal peptidase in complex with a lipopeptide-based inhibitor, J. Biol. Chem. 279 (2004) 30781–30790.
[20] M. Paetzel, R.E. Dalbey, N.C. Strynadka, Crystal structure of a bacterial signal peptidase in complex with a beta-lactam inhibitor, Nature 396 (1998) 186–190.
[21] M. Paetzel, R.E. Dalbey, N.C. Strynadka, Crystal structure of a bacterial signal peptidase apoenzyme: implications for signal peptide binding and the Ser–Lys dyad mechanism, J. Biol. Chem. 277 (2002) 9512–9519.
[22] P.A. Klenotic, J.L. Carlos, J.C. Samuelson, T.A. Schuenemann, W.R. Tschantz, M. Paetzel, N.C. Strynadka, R.E. Dalbey, The role of the conserved box E residues in the active site of the *Escherichia coli* type I signal peptidase, J. Biol. Chem. 275 (2000) 6490–6498.
[23] M.O. Kebir, D.A. Kendall, SecA specificity for different signal peptides, Biochemistry 41 (2002) 5573–55780.
[24] F. Delaglio, S. Grzesiek, G.W. Vuister, G. Zhu, J. Pfeifer, A. Bax, NMRPipe: a multidimensional spectral processing system based on UNIX pipes, J. Biomol. NMR 6 (1995) 277–293.
[25] J.L. Carlos, P.A. Klenotic, M. Paetzel, N.C. Strynadka, R.E. Dalbey, Mutational evidence of transition state stabilization by serine 88 in *Escherichia coli* type I signal peptidase, Biochemistry 39 (2000) 7276–7283.
[26] C. Zwizinski, W. Wickner, Purification and characterization of leader (signal) peptidase from *Escherichia coli*, J. Biol. Chem. 255 (1980) 7973–7977.
[27] Y. Wang, R. Bruckner, R.L. Stein, Regulation of signal peptidase by phospholipids in membrane: characterization of phospholipid bilayer incorporated *Escherichia coli* signal peptidase, Biochemistry 43 (2004) 265–270.
[28] S.J. Opella, F.M. Marassi, Structure determination of membrane proteins by NMR spectroscopy, Chem. Rev. 104 (2004) 3587–3606.
[29] H. Saito, J. Mikami, S. Yamaguchi, M. Tanio, A. Kira, T. Arakawa, K. Yamamoto, S. Tuzi, Site-directed 13C solid-state NMR studies on membrane proteins: strategy and goals toward revealing conformation and dynamics as illustrated for bacteriorhodopsin labeled with [1–13C] amino acid residues, Magn. Reson. Chem. 42 (2004) 218–230.
[30] J. Torres, T.J. Stevens, M. Samso, Membrane proteins: the 'Wild West' of structural biology, Trends Biochem. Sci. 28 (2003) 137–144.
[31] B. Bechinger, C. Aisenbrey, P. Bertani, The alignment, structure and dynamics of membrane-associated polypeptides by solid-state NMR spectroscopy, Biochim. Biophys. Acta. 1666 (2004) 190–204.
[32] X.L. Yao, M. Hong, Effects of anionic lipid and ion concentrations on the topology and segmental mobility of colicin Ia channel domain from solid-state NMR, Biochemistry 45 (2006) 289–295.
[33] M. Lorch, S. Fahem, C. Kaiser, I. Weber, A.J. Mason, J.U. Bowie, C. Glaubitz, How to prepare membrane proteins for solid-state NMR: a case study on the alpha-helical integral membrane protein diacylglycerol kinase from *E. coli*, Chembiochem. 6 (2005) 1693–1700.
[34] S. Luca, H. Heise, M. Baldus, High-resolution solid-state NMR applied to polypeptides and membrane proteins, Acc. Chem. Res. 36 (2003) 858–865.
[35] A. Watts, Solid-state NMR in drug design and discovery for membrane-embedded targets, Nat. Rev. Drug. Discov. 4 (2005) 555–568.
[36] A.A. De Angelis, S.C. Howell, A.A. Nevzorov, S.J. Opella, Structure determination of a membrane protein with two *trans*-membrane helices in aligned phospholipid bicelles by solid-state NMR spectroscopy, J. Am. Chem. Soc. 128 (2006) 12256–12267.
[37] S.H. Park, A.A. De Angelis, A.A. Nevzorov, C.H. Wu, S.J. Opella, Three-dimensional structure of the transmembrane domain of Vpu from HIV-1 in aligned phospholipid bicelles, Biophys. J. 91 (2006) 3032–3042.
[38] K. Takeuchi, M. Yokogawa, T. Matsuda, M. Sugai, S. Kawano, T. Kohno, H. Nakamura, H. Takahashi, I. Shimada, Structural basis of the KcsA K(+) channel and agitoxin2 pore-blocking toxin interaction by using the transferred cross-saturation method, Structure 11 (2003) 1381–1392.
[39] H. Inooka, T. Ohtaki, O. Kitahara, T. Ikegami, S. Endo, C. Kitada, K. Ogi, H. Onda, M. Fujino, M. Shirakawa, Conformation of a peptide ligand bound to its G-protein coupled receptor, Nat. Struct. Biol. 8 (2001) 161–165.

[40] A.L. Ulfers, J.L. McMurry, D.A. Kendall, D.F. Mierke, Structure of the third intracellular loop of the human cannabinoid 1 receptor, Biochemistry 41 (2002) 11344–11350.
[41] B. Arshava, I. Taran, H. Xie, J.M. Becker, F. Naider, High resolution NMR analysis of the seven transmembrane domains of a heptahelical receptor in organic-aqueous medium, Biopolymers 64 (2002) 161–176.
[42] A.D. Albert, P.L. Yeagle, Structural studies on rhodopsin, Biochim. Biophys. Acta. 1565 (2002) 183–195.
[43] P.L. Yeagle, A.D. Albert, Use of nuclear magnetic resonance to study the three-dimensional structure of rhodopsin, Methods Enzymol. 343 (2002) 223–231.
[44] D.F. Mierke, C. Giragossian, Peptide hormone binding to G-protein-coupled receptors: structural characterization via NMR techniques, Med. Res. Rev. 21 (2001) 450–471.
[45] F. Naider, S. Khare, B. Arshava, B. Severino, J. Russo, J.M. Becker, Synthetic peptides as probes for conformational preferences of domains of membrane receptors, Biopolymers 80 (2005) 199–213.
[46] G. Choi, J. Guo, A. Makriyannis, The conformation of the cytoplasmic helix 8 of the CB1 cannabinoid receptor using NMR and circular dichroism, Biochim. Biophys. Acta. 1668 (2005) 1–9.
[47] M. Katragadda, M.W. Maciejewski, P.L. Yeagle, Structural studies of the putative helix 8 in the human beta(2) adrenergic receptor: an NMR study, Biochim. Biophys. Acta. 1663 (2004) 74–81.
[48] P.L. Yeagle, C. Danis, G. Choi, J.L. Alderfer, A.D. Albert, Three dimensional structure of the seventh transmembrane helical domain of the G-protein receptor, rhodopsin, Mol. Vis. 6 (2000) 125–131.
[49] L. Franzoni, G. Nicastro, T.A. Pertinhez, E. Oliveira, C.R. Nakaie, A.C. Paiva, S. Schreier, A. Spisni, Structure of two fragments of the third cytoplasmic loop of the rat angiotensin II AT1A receptor. Implications with respect to receptor activation and G-protein selection and coupling, J. Biol. Chem. 274 (1999) 227–235.
[50] M. Pellegrini, M. Royo, M. Chorev, D.F. Mierke, Conformational characterization of a peptide mimetic of the third cytoplasmic loop of the G-protein coupled parathyroid hormone/parathyroid hormone related protein receptor, Biopolymers 40 (1996) 653–666.
[51] H. Jung, R. Windhaber, D. Palm, K.D. Schnackerz, Conformation of a beta-adrenoceptor-derived signal transducing peptide as inferred by circular dichroism and 1H NMR spectroscopy, Biochemistry 35 (1996) 6399–6405.
[52] D.A. Chung, E.R. Zuiderweg, C.B. Fowler, O.S. Soyer, H.I. Mosberg, R.R. Neubig, NMR structure of the second intracellular loop of the alpha 2A adrenergic receptor: evidence for a novel cytoplasmic helix, Biochemistry 41 (2002) 3596–3604.
[53] T. Lazarova, K.A. Brewin, K. Stoeber, C.R. Robinson, Characterization of peptides corresponding to the seven transmembrane domains of human adenosine A2a receptor, Biochemistry 43 (2004) 12945–12954.
[54] H. Demene, S. Granier, D. Muller, G. Guillon, M.N. Dufour, M.A. Delsuc, M. Hibert, R. Pascal, C. Mendre, Active peptidic mimics of the second intracellular loop of the V(1A) vasopressin receptor are structurally related to the second intracellular rhodopsin loop: a combined 1H NMR and biochemical study, Biochemistry 42 (2003) 8204–8213.
[55] K.H. Ruan, S.P. So, J. Wu, D. Li, A. Huang, J. Kung, Solution structure of the second extracellular loop of human thromboxane A2 receptor, Biochemistry 40 (2001) 275–280.
[56] J. Wu, S.P. So, K.H. Ruan, Solution structure of the third extracellular loop of human thromboxane A2 receptor, Arch. Biochem. Biophys. 414 (2003) 287–293.
[57] K.H. Ruan, J. Wu, S.P. So, L.A. Jenkins, C.H. Ruan, NMR structure of the thromboxane A2 receptor ligand recognition pocket, Eur. J. Biochem. 271 (2004) 3006–3016.
[58] B.W. Koenig, G. Kontaxis, D.C. Mitchell, J.M. Louis, B.J. Litman, A. Bax, Structure and orientation of a G protein fragment in the receptor bound state from residual dipolar couplings, J. Mol. Biol. 322 (2002) 441–461.
[59] J. Venkatraman, G.A. Nagana Gowda, P. Balaram, Structural analysis of synthetic peptide fragments from EmrE, a multidrug resistance protein, in a membrane-mimetic environment, Biochemistry 41 (2002) 6631–6639.
[60] P.I. Haris, Synthetic peptide fragments as probes for structure determination of potassium ion-channel proteins, Biosci. Rep. 18 (1998) 299–312.
[61] D. Askin, G.B. Bloomberg, E.J. Chambers, M.J. Tanner, NMR solution structure of a cytoplasmic surface loop of the human red cell anion transporter, band 3, Biochemistry 37 (1998) 11670–11678.
[62] M. Katragadda, J.L. Alderfer, P.L. Yeagle, Assembly of a polytopic membrane protein structure from the solution structures of overlapping peptide fragments of bacteriorhodopsin, Biophys. J. 81 (2001) 1029–1036.
[63] L.K. Tamm, H. Hong, B. Liang, Folding and assembly of beta-barrel membrane proteins, Biochim. Biophys. Acta. 1666 (2004) 250–263.
[64] T. Vosegaard, N.C. Nielsen, Towards high-resolution solid-state NMR on large uniformly ^{15}N- and [^{13}C,^{15}N]-labeled membrane proteins in oriented lipid bilayers, J. Biomol. NMR 22 (2002) 225–247.
[65] H. Hong, D.R. Patel, L.K. Tamm, B. van den Berg, The outer membrane protein OmpW forms an eight-stranded beta-barrel with a hydrophobic channel, J. Biol. Chem. 281 (2006) 7568–7577.
[66] L.K. Tamm, F. Abildgaard, A. Arora, H. Blad, J.H. Bushweller, Structure, dynamics and function of the outer membrane protein A (OmpA) and influenza hemagglutinin fusion domain in detergent micelles by solution NMR, FEBS Lett. 555 (2003) 139–143.
[67] J.H. Chill, J.M. Louis, C. Miller, A. Bax, NMR study of the tetrameric KcsA potassium channel in detergent micelles, Protein. Sci. 15 (2006) 684–698.
[68] D.S. Wishart, B.D. Sykes, F.M. Richards, Relationship between nuclear magnetic resonance chemical shift and protein secondary structure, J. Mol. Biol. 222 (1991) 311–333.
[69] D.S. Wishart, B.D. Sykes, The 13C chemical-shift index: a simple method for the identification of protein secondary structure using 13C chemical-shift data, J. Biomol. NMR 4 (1994) 171–180.
[70] Y. Wang, S. Zhao, R.L. Somerville, O. Jardetzky, Solution structure of the DNA-binding domain of the TyrR protein of *Haemophilus influenzae*, Protein. Sci. 10 (2001) 592–598.
[71] R.D. Krueger-Koplin, P.L. Sorgen, S.T. Krueger-Koplin, I.O. Rivera-Torres, S.M. Cahill, D.B. Hicks, L. Grinius, T.A. Krulwich, M.E. Girvin, An evaluation of detergents for NMR structural studies of membrane proteins, J. Biomol. NMR 28 (2004) 43–57.